

Aluminum oxide sandwiched microstructure for four-output under normal incidence

ZHICHAO XIONG, BO WANG*, YUSEN HUANG, XIAOQING ZHU, XIAOFENG WANG, HONG ZOU, JINHAI HUANG, WEIYI YU, JIAHAO LI, GUODING CHEN

School of Physics and Optoelectronic Engineering, Guangdong University of Technology, Guangzhou 510006, China

In this paper, a high-efficiency transmission four-port beam splitter grating with the incident wavelength of 800 nm under normal incidence is proposed. This grating has the characteristic of zeroth order elimination. The total diffraction efficiency of this grating achieved 89.16% and 93.40% for TE and TM polarizations respectively. Meanwhile, the beam splitter uniformity is better than 10%. We used rigorous coupled-wave analysis and the simulated annealing algorithm to calculate and optimize the parameters of the beam splitter. The fabrication tolerance of the grating is analyzed and discussed.

(Received January 14, 2022; accepted December 6, 2022)

Keywords: Four-port, Beam splitter, Transmission grating, Normal incidence

1. Introduction

Beam splitter [1-4] plays an important role in the development of optoelectronic information technology. As one of the most basic optical components, beam splitter has the advantages of high efficiency, convenience, and flexibility. It can be more effectively used in micro large-scale integrated devices, such as optical power divider [5-7], optical communication devices [8-12], image processing devices [13-16] and so on. With the development of lithography technology and micro-nano processing technology, the precision of the grating increasing constantly. As one of the most important spectroscopic elements, grating have always been a hot topic for researchers. Due to the compact volume of the grating, it can be used perfectly in micro-scale integrated optical systems, such as grating couplers [17], grating sensor [18,19], waveguide grating antenna [20], and so on.

With the unceasing development of micro-nano optical devices and grating diffraction theory, we have a systematic theoretical basis for the analysis of grating. Because of the polarization characteristics, scalar diffraction theory will lack reliability when the grating period is close to the wavelength. Rigorous coupled-wave analysis (RCWA) [21,22] and finite element method (FEM) [23-25] are the mainly types of grating vector diffraction theories. RCWA is a direct and effective electromagnetic field theory, and it strictly solves the maxwell equation in the grating region, transforms the solution of maxwell equation into a problem of solving the characteristic function, and obtains the electromagnetic field expression coupled by

the characteristic function in the grating region, and solves the boundary conditions on the interface between the grating region and other regions to obtain the final diffraction efficiency value.

While the incident light is unpolarized, the total diffraction efficiency and the polarization state of the diffraction light will be affected while the grating has polarization dependent characteristics. In many large-scale optoelectronic information systems, the polarization-independent grating is helpful to simplify the structure and improve the output capability of the system. Diffraction high dispersion and high diffraction efficiency beam splitter grating are widely used in high-power laser systems, such as the technologies of laser pulse compression [26], laser frequency selective [27,28] and spectra combined beams [29]. In recent years, researchers pay more attention in polarization-independent gratings. *Xiang* et al. proposed a single-groove grating for four-port TE polarization beam splitting under normal incidence at the wavelength of 632.8 nm. The total efficiency of the beam splitter achieved 86% with beam split uniformity better than 10% [21]. *Huang* et al. propose a single-layer sub-wavelength grating structure with beam convergence function and four-way beam splitting under the incident wavelength of 1550 nm. The calculated total transmittance for TM polarization achieved 92.67% [30].

In this paper, a sandwiched four-port transmission grating with zeroth order suppressed is proposed. The grating has a multi-layer structure to achieve the desired function. The covering layer is designed to reduce Fresnel loss. To achieve the effect of wide bandwidth, we add a connecting layer between the grating layer and the

substrate. The four-port grating presented in this paper has a good beam splitting ratio for TE and TM polarizations. The incident light is divided four beams by the grating into $\pm 1st$ and $\pm 2nd$ orders, and the 0th order is suppressed. The grating is polarization-independent, and the total efficiencies of TE polarization can achieve 89.16% and TM polarization can achieve 93.40%. Therefore, the proposed grating is a practical optical element, and has a wide application prospect.

2. The sandwiched four-port transmission grating with zeroth order suppressed

The two-dimensional and three-dimensional schematic diagram of sandwiched four-port transmission grating are shown by Fig. 1 obviously. As can be seen from Fig. 1, The grating consists of the covering layer, grating layer, connecting layer, and the substrate. The main grating parameters include the thickness of grating ridge h_1 , the thickness of connecting layer h_2 , the breadth of grating ridge b , and the period d . The grating groove is

air with refractive index of $n_1=1.0$. The material used for the grating layer, covering layer, and connecting layer are aluminum oxide, with the refractive index $n_2=1.67$. The substrate is fused silica, with refractive index of $n_3=1.45$. Duty cycle f is the ratio of b to d . The incident region is above the covering layer composed of air, and the wavelength of incident light is 800 nm.

In order to obtain the optimal parameters of the grating, a series of calculations are carried out. We analyze the data by RCWA and the simulated annealing algorithm to optimize grating parameters. The simulated annealing algorithm is a random optimization algorithm of iterative solution strategy. Ref. [31] provides the simulated annealing algorithm optimization process. The thickness of grating ridge h_1 and connecting layer h_2 are optimized to achieve higher transmission efficiencies. The depth of the grating ridge has a great influence on the phase difference of the coupled light wave. At the same time, the thickness of the connecting layer will affect the bandwidth characteristic of the grating.

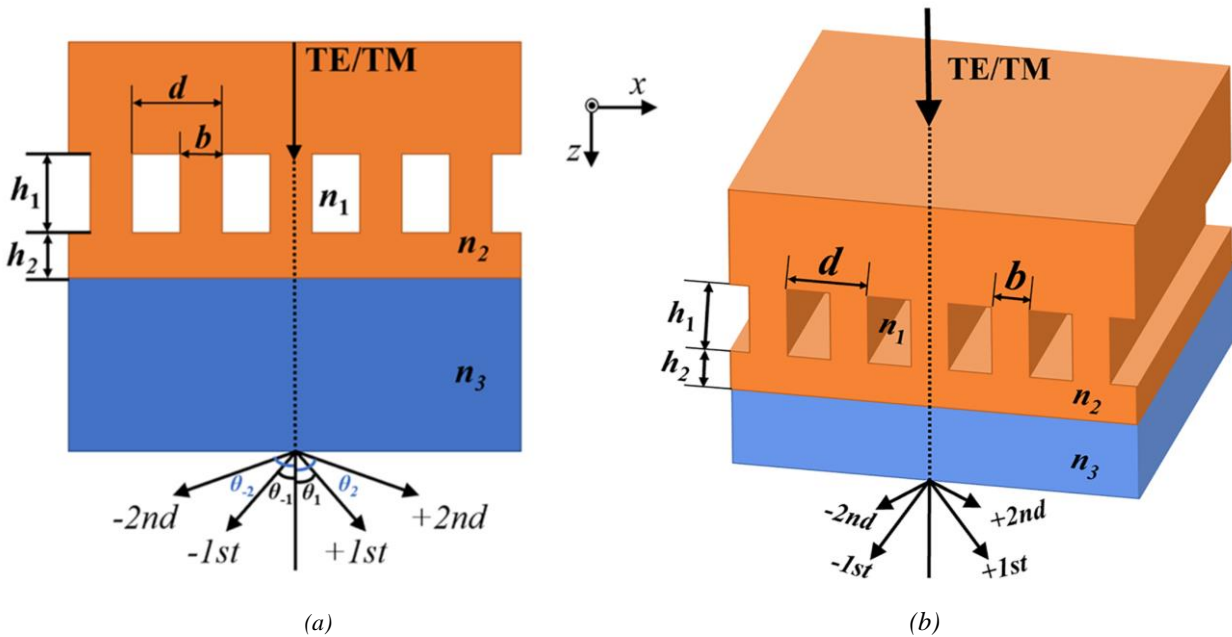


Fig. 1. Schematic of the four-port sandwiched transmission grating with zeroth order suppressed under normal incidence: (a) 2-D view (b) 3-D view (color online)

Fig. 2 demonstrates a series of contour maps of the relationship between the thickness of h_1 , h_2 and the transmission efficiency with the duty cycle of 0.4 and grating period of 1686 nm for incident wavelength of 800 nm under normal incidence. The contour maps clearly demonstrate the transmission efficiencies of the grating in $\pm 1st$ and $\pm 2nd$ orders for TE and TM polarizations. After multiple iterations of data analysis, a series of optimized parameters are obtained. According to the results we obtained, when the thickness of grating layer h_1 is 5.1 μm and the depth of connecting layer h_2 is 2.6

μm , the diffraction efficiencies of $\pm 1st$ and $\pm 2nd$ have the best performance. In this case, the transmission efficiencies for TE polarization can achieve 24.41% in the $\pm 1st$ orders and 20.17% in the $\pm 2nd$ orders. For the light of TM polarized, the transmission efficiencies of $\pm 1st$ and $\pm 2nd$ can achieve 24.96% and 21.74% respectively. The grating parameters which are obtained after a series of data analysis and calculation are listed in Table 1 integrally.

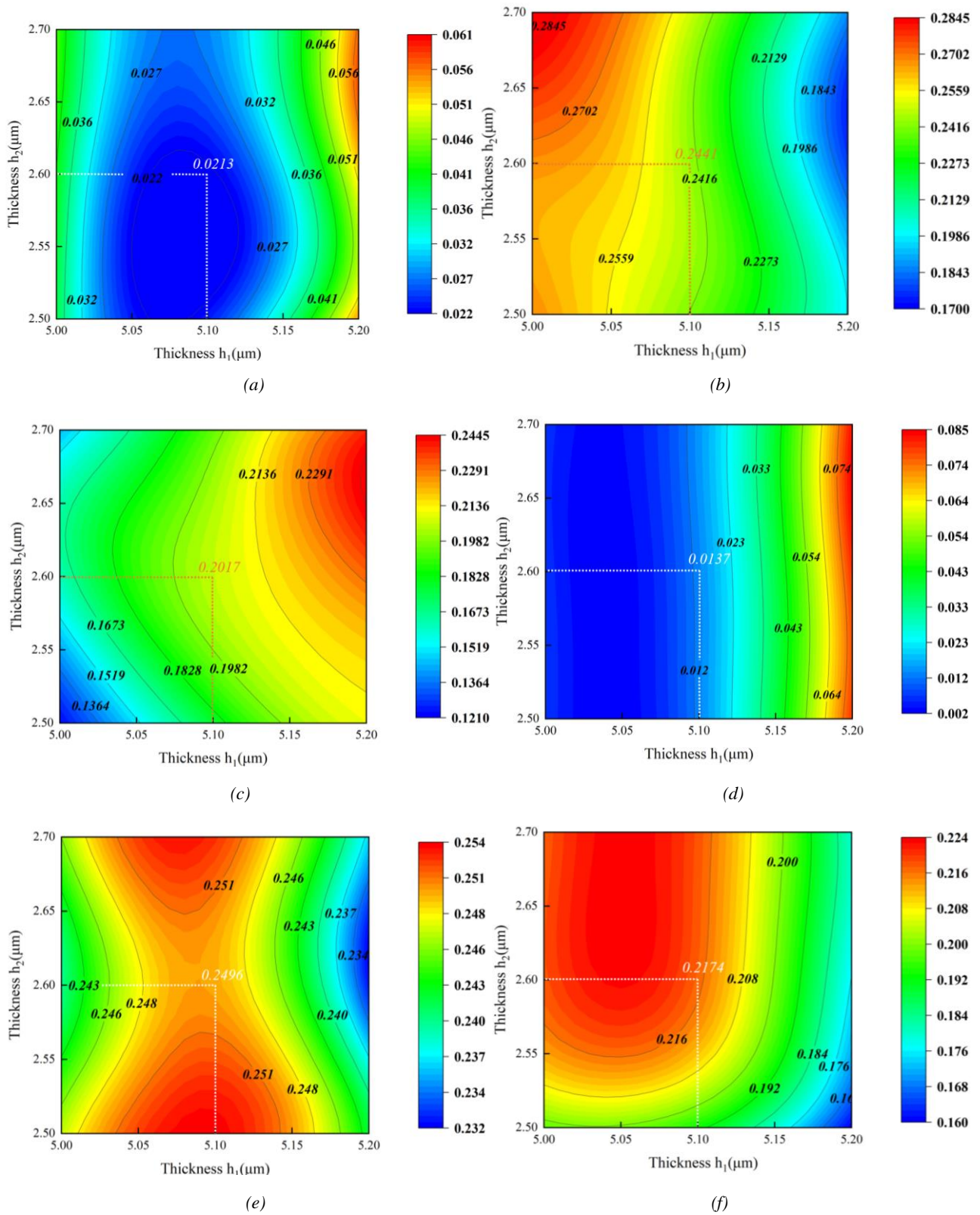


Fig. 2. The transmission efficiency versus the thickness of the grating ridge and the connecting layer depth under normal incidence with incident wavelength $\lambda=800$ nm, period $d=1686$ nm, and duty cycle $f=0.4$: (a) 0th order of TE polarization, (b) ± 1 st orders of TE polarization, (c) ± 2 nd orders of TE polarization, (d) 0th order of TM polarization, (e) ± 1 st orders of TM polarization, (f) ± 2 nd orders of TM polarization (color online)

Table 1. The optimal parameters of four-port transmission beam splitter grating with zeroth order suppressed

λ	d	f	h_1	h_2
800 nm	1686 nm	0.4	5.1 μm	2.6 μm

The distribution of normalized electric field shows the propagation path and energy distribution of incident light in the grating more directly. Fig. 3 (a) and (b) show the normalized electric field distribution of the sandwiched four-port beam splitting grating for TE and TM polarizations. It can be seen clearly from Fig. 3 that the light incident from covering layer, passes through the grating layer and connecting layer, and finally exits from the substrate. The regions closer to red indicate a larger energy distribution, while the regions closer to blue indicate a smaller energy distribution. For TE polarization, the largest energy values are distributed in the grating ridge. The grating ridge relatively shows the

characteristics of vulnerable in the manufacturing process, however, it almost has no effect on the distribution of incident light energy in the grating. It is not a rare case that the maximum energy of the incident light is distributed in the grating ridge. As shown in Refs. [32-34], when the light incident to the beam splitter gratings with different functions and parameters, the maximum energy is distributed in the grating ridge. In addition, some regions of the connection layer and the substrate also have some points of high energy distribution.

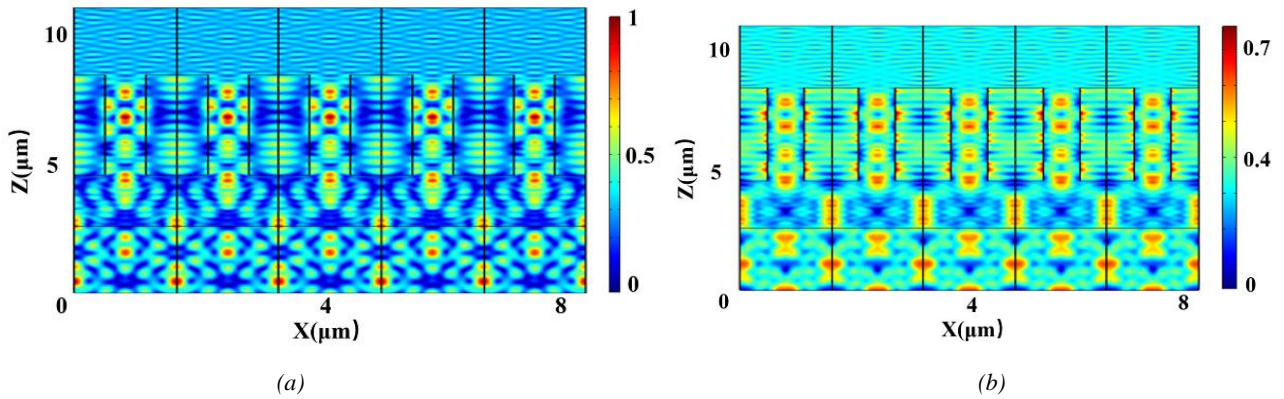


Fig. 3. Normalized electric field distribution diagram of the encapsulated grating under normal incidence: (a) TE polarization (b) TM polarization (color online)

3. Analysis and discussions

In this paper, RCWA is used to calculate and data analysis to obtain the optimum parameters. It is worth noting that under optimal parameters conditions, the TE polarization efficiency reaches 89.16% and TM polarization efficiency reaches 93.40%. However, considering the actual manufacturing process and production process, one point we must pay attention to is the redundancy of grating parameters.

The incident wavelength is an important parameter for grating. The grating performance is best when the incident wavelength is 800 nm under normal incidence. Nevertheless, the incident wavelength is not exactly 800 nm as a general rule. Fig. 4 demonstrates the relationship between incident wavelength and transmission efficiency for TE and TM polarizations under normal incidence. As shown in Fig. 4, we obtain the optimal parameter of incident wavelength after a series of optimization calculations. When the incident wavelength is 800 nm

with period of 1686 nm and duty cycle of 0.4 under normal incidence, the diffraction efficiency of the grating achieved best performance. In addition, while the incident wavelength is in the range of 790 nm to 810 nm, the diffraction efficiency of TE polarization is greater than 80%. Within this range, the zeroth order suppression efficiency of the grating is over 95% for both TE and TM polarizations. This phenomenon shows that the grating has a superior performance of zeroth order elimination within a certain range of incident wavelength.

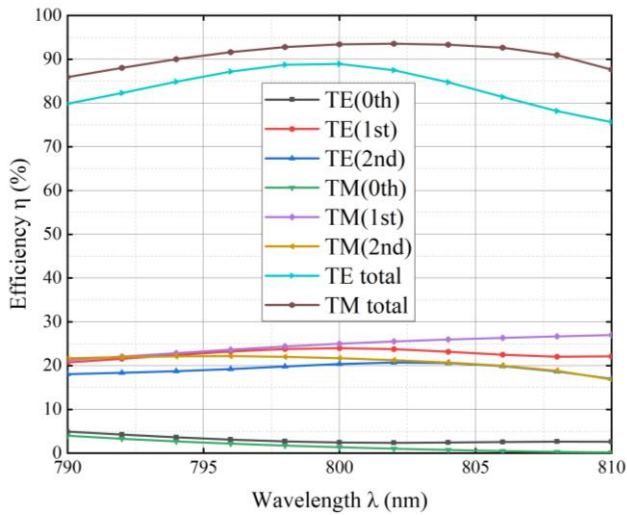


Fig. 4. The relationship between transmission efficiency and incident wavelength for both TE and TM polarizations under normal incidence with $d=1686$ nm, $f=0.4$, $h_1=5.1$ μm and $h_2=2.6$ μm (color online)

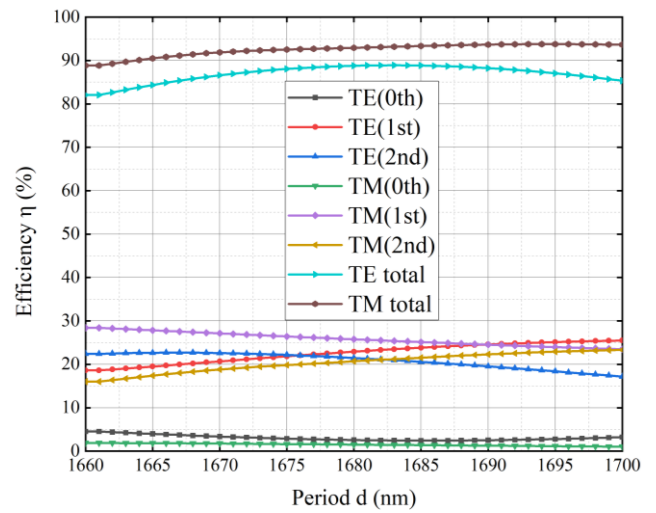


Fig. 5. Diffraction efficiency at different period for both TE and TM polarizations under normal incidence with incident wavelength $\lambda=800$ nm, duty cycle $f=0.4$, $h_1=5.1$ μm , $h_2=2.6$ μm (color online)

What's more, period is also a major factor affecting the diffraction efficiency of the grating. In theory, the period of the designed grating is certain. However, due to the actual manufacturing process and technology, grating period is often not accurate to an exact value. In many cases, a slight change of the grating period can cause a huge difference in the performance of the grating. Therefore, finding the tolerance value of grating period is of great significance to the research of grating. The transmission efficiencies of TE and TM polarizations versus period is shown in Fig. 5. As illustrated in Fig. 5, we obtain the results that the diffraction efficiency is greatest when the period is set to 1686 nm. It can be seen from Fig. 5 that when the period is in the range of 1676 nm to 1687 nm, the diffraction efficiencies of ± 1 st and ± 2 nd orders for TE and TM polarizations are exceed 20%. In the meantime, when the period is in the range of 1674 nm to 1697 nm, the zeroth order suppression efficiency of the grating is over 97%. The tolerance of grating period is considered to be beneficial to grating processing.

Fig. 6 demonstrates the diffraction efficiency versus the duty cycle with grating period of 1686 nm under normal incidence. The value of duty cycle is closely related to the processing technology. As we can see from the Fig. 6, the diffraction efficiency of grating is optimal when the duty cycle is set to 0.4. Within a certain tolerance range, the diffraction efficiencies of ± 1 st and ± 2 nd orders still more than 20% for both TE and TM polarizations while the duty cycle is in the range of 0.39 to 0.41.

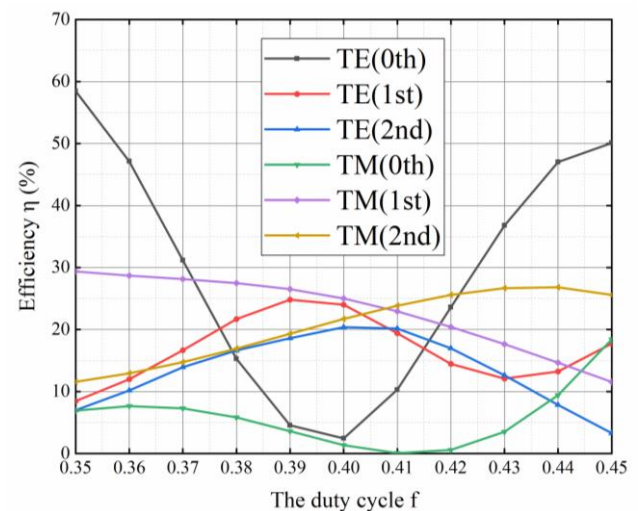


Fig. 6. Diffraction efficiency at a range of duty cycle for both TE and TM polarizations under normal incidence with incident wavelength $\lambda=800$ nm, period $d=1686$ nm, $h_1=5.1$ μm , $h_2=2.6$ μm (color online)

To ensure the accuracy of the optimal parameter, we use FEM to verify the obtained data. Table 2 clearly illustrates the diffraction efficiencies of the grating obtained by FEM and RCWA of TE and TM polarizations at ± 1 st orders and ± 2 nd orders, respectively.

It can be seen from the table that the calculated results obtained by FEM and RCWA are consistent. The comparison shows the accuracy of the optimal parameters.

Table 2. The transmission efficiencies of the grating obtained by FEM and RCWA for TE polarization and TM polarization with period $d = 1686$ nm, incident wavelength $\lambda = 800$ nm, duty cycle $f = 0.4$, $h_1 = 5.1$ μ m, $h_2 = 2.6$ μ m

Polarization	0th	± 1 st	± 2 nd
TE (FEM)	2.44%	24.03%	20.38%
TE (RCWA)	2.13%	24.41%	20.17%
TM (FEM)	1.35%	25.00%	21.70%
TM (RCWA)	1.37%	24.96%	21.74%

The grating we proposed has the characteristic of high beam splitting efficiency. The total efficiency of the sandwiched four-port beam splitter grating with zeroth order suppressed achieve 89.16% and 93.40% for TE and TM polarizations with beam splitting uniformity better than 10%. The performance of the grating is significantly better than the four-port beam splitter grating proposed from Ref. [21], which just achieve the total efficiency of 86%. In addition, for TM polarization, the efficiency of a four-port beam splitter grating presented by Ref. [27] is achieved 92.67%. However, the beam splitting efficiency of the grating proposed in this paper reaches 93.4% and has a wider period bandwidth. Therefore, the proposed grating is of great significance to many micro-nano optical elements and systems.

4. Conclusion

In this paper, a sandwiched four-port transmission grating with zeroth order suppressed under normal incidence is proposed. According to RCWA and verify with FEM, the optimized parameters of the beam splitter grating are calculated and the results are satisfactory. For TE polarization, the efficiencies of ± 1 st and ± 2 nd orders are achieved 24.41% and 20.17% respectively. In the meantime, the diffraction efficiencies of ± 1 st orders for TM polarization can achieve 24.96%, with the efficiencies of ± 2 nd orders are greater than 21%. Moreover, in order to calculate the tolerance of the grating, the relationship between transmission efficiency and duty cycle, incident wavelength, and period are analyzed. The results of analysis indicate that the grating can achieve the effect of four-port transmission-type beam splitter with the elimination of zeroth order. In addition, the proposed grating has the characteristic of broad incident wavelength bandwidth for TE and TM polarization. Therefore, the grating presented in this paper has a broad application prospect in the field of micro-nano optical devices.

Acknowledgements

This work is supported by the Science and Technology Program of Guangzhou (202002030284, 202007010001).

References

- [1] B. Zhou, W. Jia, C. Xiang, Y. Xie, J. Wang, G. Jin, Y. Wang, C. Zhou, *Opt. Express* **29**(20), 437974 (2021).
- [2] P. Pan, J. Wen, S. Zha, X. Cai, H. Ma, J. An, *Opt. Mater.* **118**, 111250 (2021).
- [3] J. Zhang, X. Chen, F. Zuo, L. Liu, W. Zhao, Z. Zhang, X. Song, K. Guo, *Opt. Commun.* **493**, 126814 (2021).
- [4] D. Liu, D. S. Citrin, S. Hu, *Opt. Mater.* **109**, 110256 (2020).
- [5] J. Huang, Q. Ye, H. Jin, *Opt. Laser. Eng.* **129**, 106051 (2020).
- [6] Y. Zheng, B. Xia, L. Jiang, X. Wu, J. Duan, *Optik* **217**, 164890 (2020).
- [7] U. F. S. Roggero, H. E. Hernández-Figueroa, *Opt. Laser Technol.* **127**, 106127 (2020).
- [8] C. Wang, T. Ning, J. Li, L. Pei, J. Zheng, C. Xie, X. Dong, *Opt. Laser Technol.* **136**, 106731 (2021).
- [9] J. Chen, D. Gao, *Optik* **220**, 165131 (2020).
- [10] P. A. Mohammed, *Opt. Mater.* **111**, 110685 (2021).
- [11] D. A. Presti, V. Guarepi, F. Videla, G. A. Torchia, *Opt. Laser. Eng.* **126**, 105860 (2020).
- [12] N. Jellali, M. Ferchichi, M. Najjar, *Optik* **244**, 166188 (2021).
- [13] Z. Huang, B. Wang, Z. Lin, K. Wen, Z. Meng, F. Zhang, Z. Nie, X. Xing, L. Chen, L. Lei, J. Zhou, *Optik* **242**, 167289 (2021).
- [14] Z. Chen, R. Meng, Y. Zhu, H. Ma, *Opt. Laser. Eng.* **129**, 106055 (2020).
- [15] Y. Liu, Q. Liu, Y. Li, J. Zhang, Z. He, *Opt. Laser. Eng.* **140**, 106530 (2021).

- [16] M. S. Pandian, S. Verma, P. Pareek, P. Ramasamy, K. S. Bartwal, *Opt. Laser Technol.* **132**, 106491 (2020).
- [17] P. Sanati, A. Shafiee, M. Bahadoran, E. Akbari, *Eur. Phys. J. Plus* **135**(11), 869 (2020).
- [18] G. Pesce, P. H. Jones, O. M. Maragò, G. Volpe, *Eur. Phys. J. Plus* **135**(12), 949 (2020).
- [19] J.-X. Liu, Y. Jiang, L.-H. Ming, W.-C. Tang, H.-W. Yang, *Eur. Phys. J. Plus* **135**(10), 805 (2020).
- [20] G. Wu, Y. Huang, X. Duan, K. Liu, X. Ma, T. Liu, H. Wang, X. Ren, *Opt. Commun.* **456**, 124458 (2020).
- [21] C. Xiang, C. Zhou, W. Jia, J. Wang, *Proc. SPIE* **10818**, 1081812 (2018).
- [22] G. G. Zheng, P. Zhou, Y. Y. Chen, *Opt. Mater.* **99**, 109581 (2020).
- [23] B. Ali, S. Hussain, S. Abdal, M. M. Mehdi, *Eur. Phys. J. Plus* **135**(10), 821 (2020).
- [24] Ö. Civalek, B. Uzun, M. Ö. Yaylı, B. Akgöz, *Eur. Phys. J. Plus* **135**(4), 381 (2020).
- [25] M. Fakher, S. Behdad, S. Hosseini-Hashemi, *Eur. Phys. J. Plus* **135**(11), 905 (2020).
- [26] H. Wang, W. Luan, X. Yan, *Optik* **247**, 167871 (2021).
- [27] S. Farhadi, M. Miri, A. Alighanbari, *Appl. Phys. B-Lasers O.* **126**(7), 118 (2020).
- [28] C. Fu, B. Wang, J. Fang, K. Wen, Z. Meng, Q. Wang, Z. Nie, X. Xing, L. Chen, L. Lei, J. Zhou, *Optoelectron. Adv. Mat.* **14**(7-8), 297 (2020).
- [29] Y. Chen, J. Xiao, *Opt. Eng.* **59**(1), 017101 (2020).
- [30] C. Huang, C. Bai, W. Fang, X. Fan, X. Jiang, *Laser Optoelectron. P.* **57**(3), 030502 (2020).
- [31] J. Wu, C. Zhou, H. Cao, A. Hu, J. Yu, W. Sun, W. Jia, *J. Opt.* **13**(11), 115703 (2011).
- [32] C. Fu, B. Wang, *Laser Phys.* **31**(11), (2021).
- [33] Z. Lin, B. Wang, K. Wen, *Opt. Commun.* **505**, 127499 (2022).
- [34] Z. Lin, B. Wang, C. Fu, *Phys. Scripta* **96**(12), (2021).

*Corresponding author: wangb_wsx@yeah.net